Available online at www.sciencedirect.com

SCIENCE DIRECT®

Earth and Planetary Science Letters 237 (2005) 33–44

EPSL

www.elsevier.com/locate/epsl

Final closure of Panama and the onset of northern hemisphere glaciation

G. Bartoli [a,*], M. Sarnthein [a], M. Weinelt [a], H. Erlenkeuser [b], D. Garbe-Schönberg [a], D.W. Lea [c]

[a] *Kiel University, Institute for Geosciences, Olshausenstr. 40, D-24118 Kiel, Germany*
[b] *Leibniz-Laboratory for Radiometric Dating and Stable Isotope Research, Kiel University, Max-Eyth-Str. 11, D-24118 Kiel, Germany*
[c] *Department of Geological Sciences, University of California, Santa Barbara, CA 93106, USA*

Received 26 November 2004; received in revised form 10 May 2005; accepted 10 June 2005
Available online 21 July 2005
Editor: E. Boyle

Abstract

The Greenland ice sheet is accepted as a key factor controlling the Quaternary "glacial scenario". However, the origin and mechanisms of major Arctic glaciation starting at 3.15 Ma and culminating at 2.74 Ma are still controversial. For this phase of intense cooling Ravelo et al. [1] [A.C. Ravelo, D.H. Andreasen, M. Lyle, A.O. Lyle, M.W. Wara, Regional climate shifts caused by gradual global cooling in the Pliocene epoch. Nature 429 (2004) 263–267.] proposed a complex gradual forcing mechanism. In contrast, our new submillennial-scale paleoceanographic records from the Pliocene North Atlantic suggest a far more precise timing and forcing for the initiation of northern hemisphere glaciation (NHG), since it was linked to a 2–3 °C surface water warming during warm stages from 2.95 to 2.82 Ma. These records support previous models [G.H. Haug, R. Tiedemann, Effect of the formation of the Isthmus of Panama on Atlantic Ocean thermohaline circulation, Nature 393 (1998) 673–676.[2]] claiming that the final closure of the Panama Isthmus (3.0– ~2.5 Ma [J. Groeneveld S. Steph, R. Tiedemann, D. Nürnberg, D. Garbe-Schönberg, The final closure of the Central American Seaway, Geology, in prep. [3]]) induced an increased poleward salt and heat transport. Associated strengthening of North Atlantic Thermohaline Circulation and in turn, an intensified moisture supply to northern high latitudes resulted in the build-up of NHG, finally culminating in the great, irreversible "climate crash" at marine isotope stage G6 (2.74 Ma). In summary, there was a two-step threshold mechanism that marked the onset of NHG with glacial-to-interglacial cycles quasi-persistent until today.

Keywords: Late Pliocene; onset of NHG; foraminiferal Mg/Ca; Panama closure

* Corresponding author. Tel.: +49 4318802884; fax: +49 4318804376.
E-mail address: gb@gpi.uni-kiel.de (G. Bartoli).

0012-821X
doi:10.1016/j.epsl.2005.06.020

1. Introduction

Pleistocene climate is characterized by a persistent succession of glacial-to-interglacial cycles driven by orbital forcing. However, these northern hemisphere glaciations (NHG) and large-scale Arctic sea ice have only appeared since the Late Pliocene (~3.2 Ma), a time, when a major reorganization of the ocean-climate system took place. This event appears approximately coeval with the final closure of the Central American Seaways (CAS) ending the advection of Pacific surface water into the Atlantic Ocean [3,4]. In this context, two questions are still controversial, (1) the precise timing of the final closure of the CAS and (2), whether a causal relationship exists between this closure and the onset of NHG and to which physical processes it may be ascribed [1].

Whereas intermediate-water circulation through the Panama Strait was gradually barred as early as 4.5–4.0 Ma with short-lasting re-openings near 3.8 and 3.4–3.3 Ma [2,5], a shallow-water connection continued far beyond 3.0 Ma [6]. This gateway ensured the advection of Pacific low-salinity surface water into the southern Caribbean, here weakening the North Atlantic salt transport. Combined $\delta^{18}O$ and Mg/Ca records of *Globigerinoides sacculifer* used as proxy of surface water salinity at south Caribbean Site 999 [3,7] depict a first weak divergence of 0.0–0.4‰ $\delta^{18}O$ between Caribbean and Pacific sea surface salinity (SSS) records at 4.0–3.8 Ma. However, this minor offset remained constant further on, with a significant short-term convergence near 3.3 Ma. Only thereafter, we observe a second, renewed divergence with a $\delta^{18}O$ offset, finally reaching 1‰ at 2.5 Ma, a divergence that is crucial for question (2), the potential processes in the ocean and atmosphere, that have led to NHG.

One model [8] suggests that the closure of the CAS has enhanced the advection of warm and saline water to northern high-latitudes which, in turn, increased North Atlantic Deep Water (NADW) production. This process led to higher evaporation and hence to more moisture supply to high latitudes, fueling the build-up of northern hemisphere ice-sheets. Increasing amplitude variations of Earth obliquity leading to periods with colder summers may have transformed the additional moisture into a permanent snow cover [2]. The orbital trend, however, has been reversed after 2.2 Ma, whereas the Greenland ice sheet remained in place ever since and has acted as key albedo factor for the enhanced climate sensitivity to orbital forcing, characteristic of the Quaternary. Driscoll and Haug [9] postulate a different suite of processes, proposing that increased delivery of freshwater to the Arctic Ocean via the Siberian rivers has promoted formation of sea ice, enhancing the albedo thus cooling the North Polar region. However, pertinent records are still lacking.

To trace back potential changes in THC between 3.2 to 2.5 Ma, that may have served as trigger for NHG, we now present new submillennial-scale records of Mg/Ca-paleothermometry and stable isotopes from planktic and benthic foraminifers in the northern North Atlantic, a region crucial for the understanding of NHG (Fig. 1).

2. Study area and methods

ODP 984 (61.25°N, 24.04°W, 1648 m, Bjorn Drift) records the history of the Irminger Current (IC) and LSW (Labrador Sea Water, Upper NADW). DSDP 609 (49.52°N, 24.14°W, 3883 m, eastern flank of the Mid-Atlantic Ridge) records changes in NAC (North Atlantic Current), SSW (Southern Source Water), and in Lower NADW (LNADW).

2.1. Age control

At Site 984, magnetic stratigraphy suffered from drilling disturbance below 260 mbsf, at the base of the advanced hydraulic piston corer (APC) section [10] and thus was only measured back to 2.2 Ma (Reunion). Further back, biostratigraphic control was established by the last occurrence (LO) of *Ebriopsis cornuta* between 359.74 to 369.06 mbsf (2.61 Ma). In absence of any benthic $\delta^{18}O$ record, Raymo tried to deduce a succession of marine isotope stages from the magnetic susceptibility record [11]. Proceeding from her estimates we established a revised stable-isotope stratigraphy using our new isotopic records of *Globigerina bulloides* and *Neogloboquadrina atlantica* and mixed benthic species (Fig. 2). This stratigraphic framework is compared with planktic and benthic isotopic records from Site 610 on the Rockall Plateau [12], much farther south, records

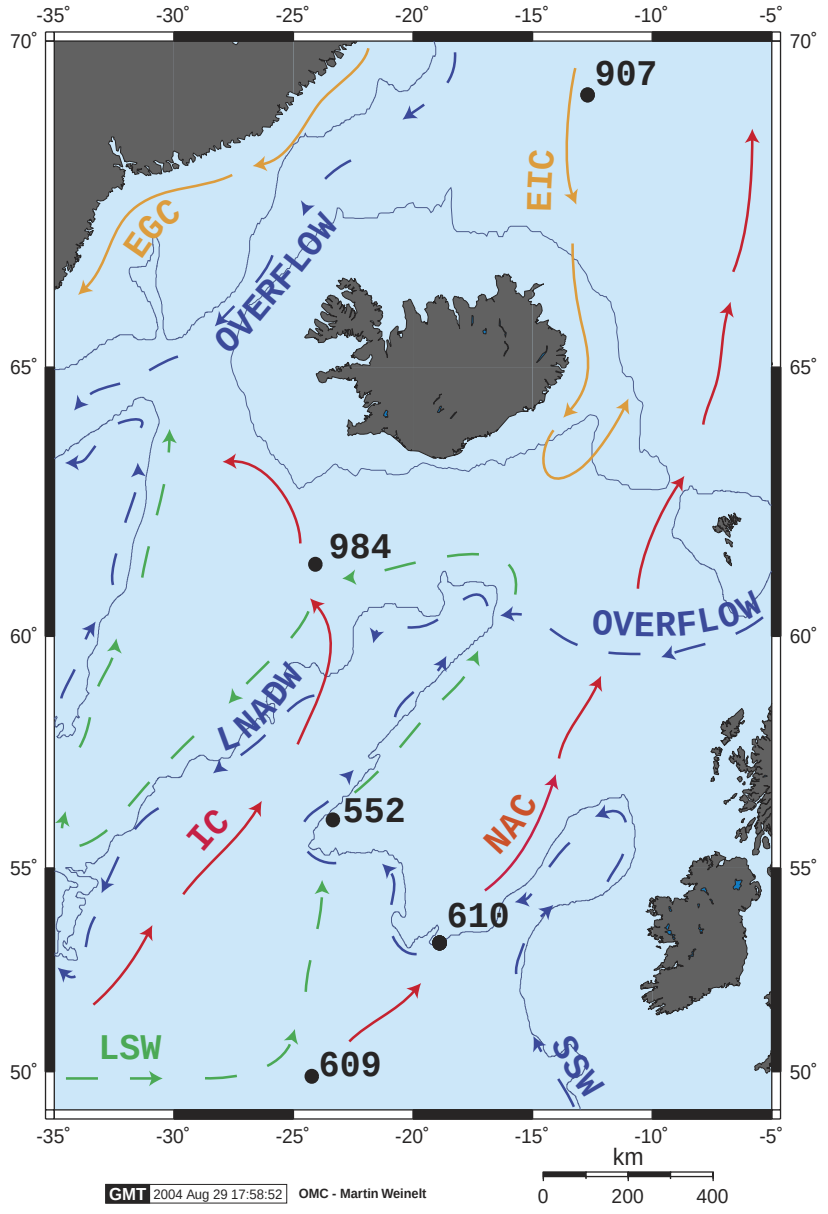

Fig. 1. Site locations (numbers) and modern surface (solid lines) and deep-water currents (broken lines) in the Northeast Atlantic. IC stands for Irminger Current, NAC for North Atlantic Current, EGC for East Greenland Current, EIC for East Iceland Current LSW for Labrador Sea Water, SSW for Southern Source Water, and NADW for North Atlantic Deep Water.

that extend back to MG6 (3.5 Ma), however, with a much lower resolution.

Direct orbital tuning could not be employed because of glacial-to-interglacial changes in sedimentation rate and various gaps in the records because of samples barren of foraminifers. Instead, age models of ODP 984 and DSDP 609 are based on magneto- and biostratigraphic control points defined by the DSDP/ODP shipboard parties and on detailed tuning of the planktic $\delta^{18}O$ (ODP 984) and benthic $\delta^{18}O$ (DSDP 609) records to the standard benthic $\delta^{18}O$ stratigraphy of ODP 846 [13]. Time resolution at ODP 984 gen-

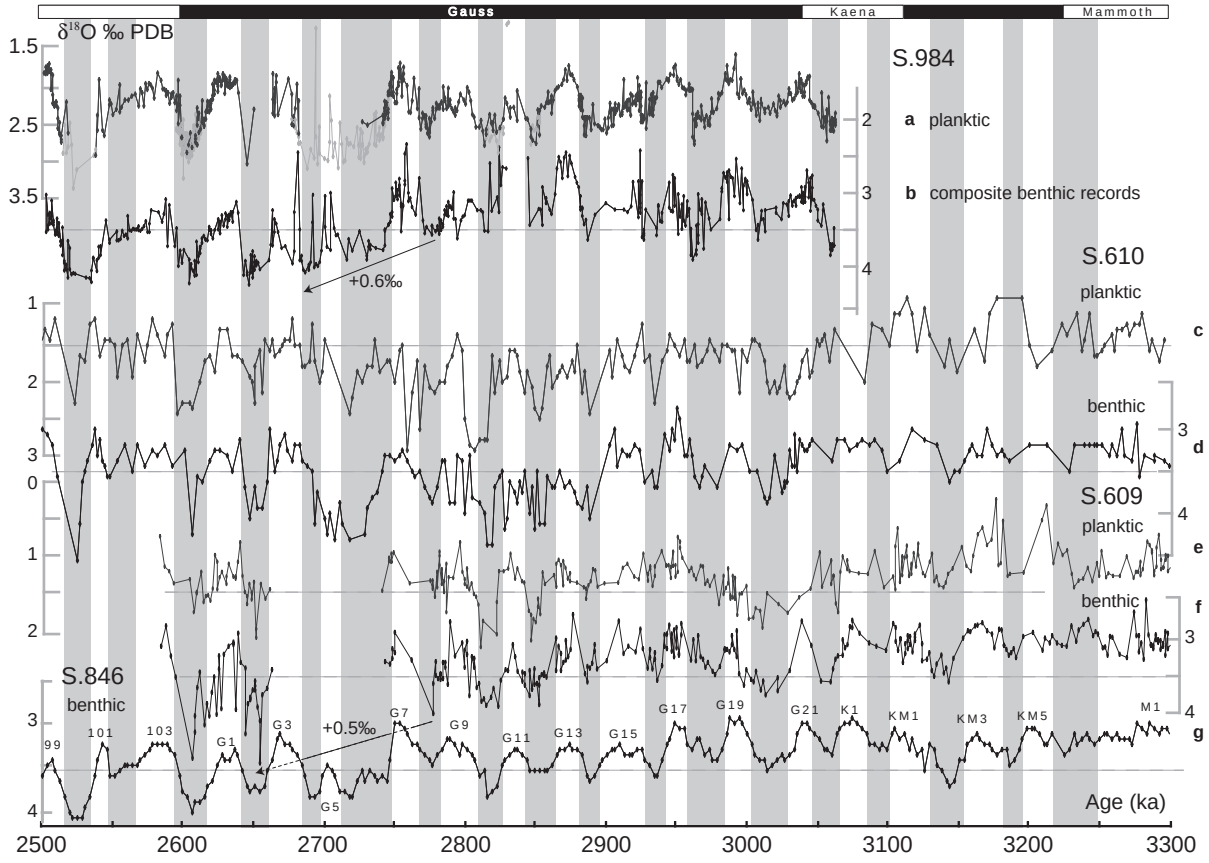

Fig. 2. Age control based on planktic and benthic $\delta^{18}O$ records fitted to the orbitally tuned benthic record [13] of ODP 846. (a) Planktic $\delta^{18}O$ record from ODP 984. Dark grey diamonds present data based on *G. bulloides* and light grey diamonds data based on *N. atlantica.* (b) Benthic $\delta^{18}O$ from ODP 984 based on multiple foraminiferal species (see Methods). Arrows indicate long-term shift in glacial $\delta^{18}O$ level from MIS G8 to MIS G4. (c) Planktic $\delta^{18}O$ record from DSDP 610 [12]. (d) Benthic $\delta^{18}O$ record from DSDP 610 [12]. (e) Planktic $\delta^{18}O$ record from DSDP 609, based on *G. bulloides*. (f) Benthic $\delta^{18}O$ from DSDP 609 based on multiple foraminiferal species (see Methods). Data for MIS G17 to M2 from R. Tiedemann (unpubl.). (g) Composite benthic $\delta^{18}O$ from ODP 846 [13]. Numbers 101, 103, G1, etc., indicate interglacial Marine Isotope Stages.

erally amounts to 300–600 yrs. This unprecedented sampling resolution for Late Pliocene records enables us to compare millennial-scale climate changes prior and after the onset of NHG.

2.2. Stable isotope and Mg/Ca analysis

Monospecific samples for stable isotopes analyses usually consist of 1 to 5 benthic foraminifers (Table 1) and 1 to 30 *G. bulloides* specimens. They were sonicated in ethanol for 5–10 s, oven dried at 40 °C, and measured on the Kiel Device I/Finnigan MAT251 system with an analytical precision of 0.07‰ for $\delta^{18}O$ and 0.05‰ for $\delta^{13}C$ at the Leibniz Laboratory in Kiel. Benthic $\delta^{18}O$ and $\delta^{13}C$ values were corrected for species-specific offsets relative to *Uvigerina peregrina* and *Cibicides wuellerstorfi*, considered to represent equilibrium $\delta^{18}O$ and $\delta^{13}C$, respectively, listed in Table 1.

Foraminiferal samples for Mg/Ca analyses were cleaned according to the protocol of Martin and Lea [18]. Analyses were partly performed at University of California in Santa Barbara (UCSB) on an ICP-SF-MS instrument (Thermo Finnigan Element). Most samples were analyzed at the Institute of Geosciences of Kiel University [19], using a simultaneous ICP-

Table 1
Benthic foraminifer species used for stable isotopes measurements and correction applied for species-specific offsets relative to *U. peregrina* and *C. wuellerstorfi* considered to represent equilibrium $\delta^{18}O$ and $\delta^{13}C$, respectively

	$\delta^{18}O$	$\delta^{13}C$	References
Cibicides wuellerstorfi	+0.64	0.00	[14]
Cibicides pachyderma	+0.64	0.00	[14]
Uvigerina peregrina	0.00	not used	[14]
Oridorsalis tener	0.00	not used	[14]
Elphidium excavatum	+0.64	not used	[15]
Cassidulina teretis	0.00	not used	[16]
Melonis barleeanum	+0.36	not used	[17]

OES instrument (Spectro Ciros SOP) with cooled cyclonic spraychamber and microconcentric nebulization (200 $\mu l.min^{-1}$). Intensity ratio calibration followed the method of de Villiers et al. [20]. Internal analytical precision at Kiel and UCSB labs was estimated from replicate measurements and is better than 0.1–0.2% RSD corresponding to ± 0.02 °C. Replicate analyses on the same samples (cleaned and re-analyzed) showed a standard deviation of 0.09 mmol/mol, equivalent to a temperature error of 0.5 °C. Accuracy was checked by analyzing sets of consistency standards obtained from M. Greaves, University of Cambridge, and D. Lea, UCSB. Differences in molar Mg/Ca between the labs were $\pm 1\%_{rel}$.

Paleo-sea surface temperatures (SST) were derived from the Mg/Ca ratio using the calibration curves of Mashiotta et al. [21] for *G. bulloides* (± 0.8 °C). Since no specific calibration exists for *N. atlantica*, a species that became extinct at 1.8 Ma, and since using the calibration for its potential descendant *N. pachyderma* sin. may introduce some bias [22], we used the multispecies calibration of Elderfield and Ganssen [23] calculated for eight North Atlantic planktic species (including *N. pachyderma* sin.) as suggested by Anand et al. [24], where the overall calibration accuracy is ± 0.7 °C.

Deepwater temperatures (DWT) were obtained from five benthic foraminiferal species. Large parts of the DWT record employ the average of Mg/Ca-based temperature values measured on up to five different species with the intent to overcome the calibration uncertainties of single-species records. Individual calibration curves were used from Martin et al. [25] for *U. peregrina*, and from Lear et al. [26] for *Melonis barleeanuum, C. wuellerstorfi, Oridorsalis umbonatus*, and *C. pachyderma.* Calibration accuracy is ± 1.4 °C and ± 1 °C, respectively.

Ice volume was deduced from benthic $\delta^{18}O$ after correction for DWT assuming constant deepwater salinity, with 0.1‰ seawater $\delta^{18}O$ set equal to 10 m sea level [27].

In addition, census counts of selected benthic foraminifera species indicating environmental change were performed on the size fraction larger than 150 microns. Since many samples contain very low specimen numbers, only raw census data (individuals per 10 g dry sediment) are shown.

3. Results and discussion

3.1. The Late Pliocene "*climate crash*"

The first occurrence of continental-scale ice sheets, especially on Greenland, is recorded as ice-rafted detritus (IRD) released from drifting icebergs into sediments of the mid- and high-latitude ocean. After a transient precursor event at 3.2 Ma, signals of large-scale glaciations suddenly started in the subpolar North Atlantic in two steps, at 2.92–2.82 and 2.74–2.64 Ma, that are Marine Isotopes Stages (MIS) G16-G10 and G6-G2 (e.g [28–30,12]) (Fig. 3a). The latter interval is also recorded for the onset of IRD deposition in the North Pacific [31].

This largely irreversible "climate crash" is also reflected by a profound and rapid reorganization of the northern high-latitude faunal provinces. For example, Atlantic planktic foraminiferal high-latitude provinces shifted dramatically southward while low-latitude provinces contracted [32]. In the Northwest Pacific, the proportion of *Coccolithus pelagicus*, today a typical cold-water phytoplankton species, jumped to 80% at 2.74 Ma [33]. This event is linked to the onset of NHG and precisely coeval with the separation of Pacific and Caribbean coccolithophorid assemblages, which results from the final closure of the Panama Isthmus [34].

The benthic foraminifer *Cassidulina teretis* which is adapted to low nutrients, harsher over-all conditions, and perhaps to higher seasonality became dominant at Rockall Plateau (DSDP 552) along with the first occurrence of IRD and cold-water planktic foraminifers [35]. Our new centennial-scale record of

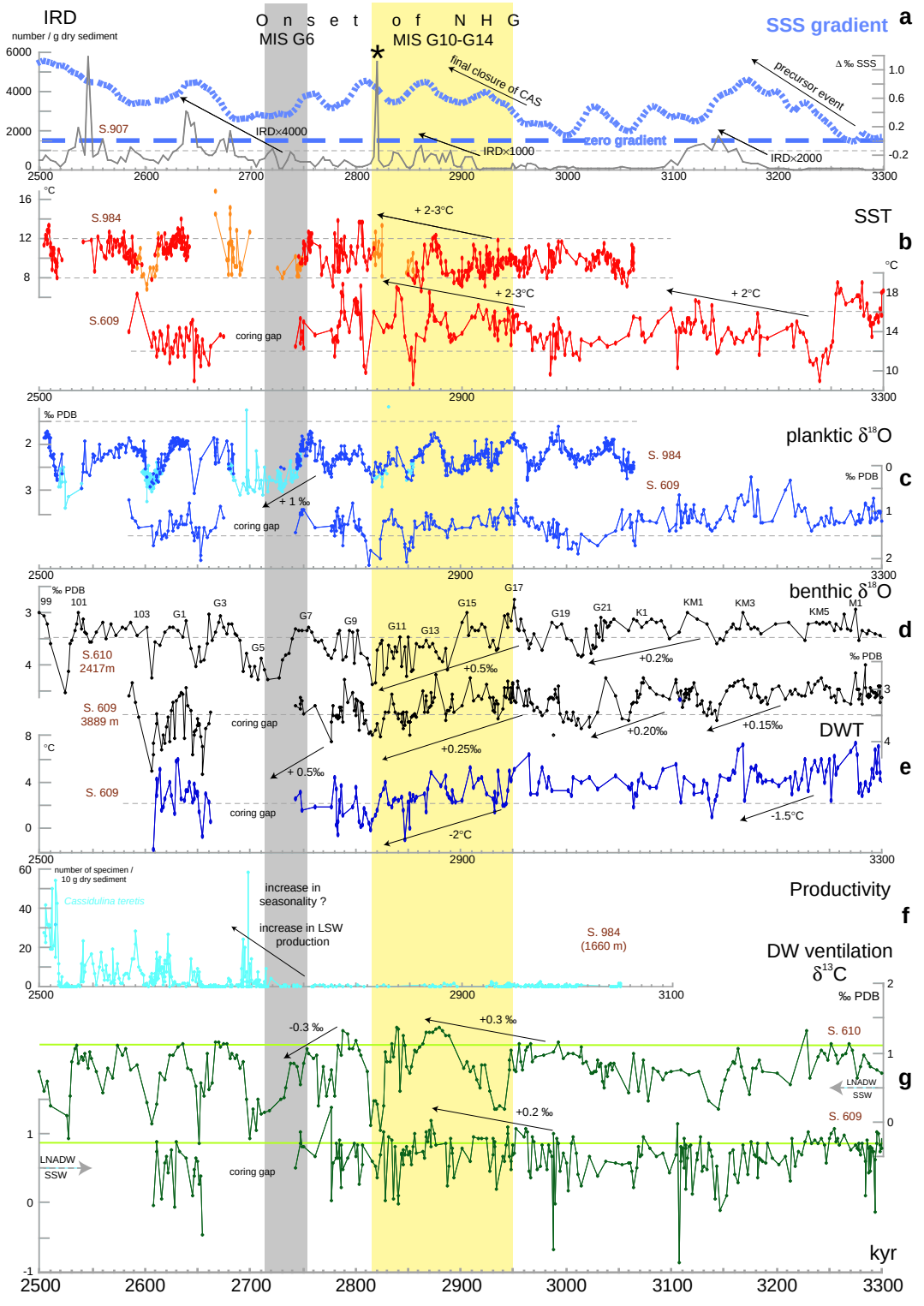
IRD
number / g dry sediment
Onset of NHG
MIS G6
MIS G10-G14
SSS gradient
a
final closure of CAS
precursor event
Δ ‰ SSS
S.907
IRD×4000
IRD×1000
zero gradient
IRD×2000
SST
b
S.984
+ 2-3°C
+ 2°C
S.609
coring gap
planktic δ18O
c
S. 984
S. 609
+ 1 ‰
benthic δ18O
d
S.610
2417m
S. 609
3889 m
+0.5‰
+0.2‰
+0.20‰
+0.15‰
+0.25‰
DWT
e
+ 0.5‰
-2°C
-1.5°C
Productivity
f
number of specimen / 10 g dry sediment
Cassidulina teretis
increase in seasonality ?
increase in LSW production
S. 984
(1660 m)
DW ventilation
δ13C
‰ PDB
g
-0.3 ‰
+0.3 ‰
+0.2 ‰
S. 610
S. 609
LNADW
SSW
kyr

ODP 984 now defines the sudden dominance of *C. teretis* in the Upper NADW level and the rapid reorganization of the North Atlantic THC at precisely 2.74 Ma (Fig. 3f).

The major expansion of global ice volume over MIS G16–G10 (2.93–2.82 Ma) is widely reflected in paleoceanographic records by a benthic 0.4‰ $\delta^{18}O$ increase [36,37]. In North Atlantic deepwater, the total increase from 3.2–2.8 Ma was stronger, amounting to 0.7‰ (Fig. 3d) which also documents a long-term cooling trend as deduced from ostracods [38] and from benthic foraminiferal Mg/Ca (Fig. 3e). Changes in North Atlantic DWT (DSDP 609) largely parallel the benthic $\delta^{18}O$ variations and range from −1.8° to 7.4 °C, that is between temperatures as cold as in the modern Nordic Seas and temperatures that were ~4–5 °C warmer than today. Between 2.94 and 2.81 Ma, average DWT decreased by 2 °C during both glacials and interglacials. This trend is consistent with a Late Pliocene ~4 °C cooling recorded at ODP 747 (Southern Ocean, ~1700 m) [39] and a global average cooling of deepwater by ~3.5 °C from 5 Ma to today [40].

To better constrain the role of the THC over this critical time span, we employed three benthic $\delta^{18}O$ records from different water depths in the northeastern Atlantic (Fig. 2). On the basis of coeval strong $\delta^{13}C$ oscillations the benthic $\delta^{18}O$ records at DSDP 609 (3900 m water depth) and DSDP 610 (2400 m water depth) [12] reveal an alternating glacial-to-interglacial influence of SSW and LNADW in addition to global ice volume and DWT changes.

In summary, Mg/Ca-based DWT record a coeval stepwise cooling by at least 2 °C, equal to a 0.45–0.55‰ $\delta^{18}O$ increase (Fig. 3e). The remaining benthic $\delta^{18}O$ increase by 0.2‰ suggests a growth of global ice volume during glacial stages equivalent to 20–25 m sea level drop. A further drop by 20 m (equivalent to 0.2‰ $\delta^{18}O$) should be added to compensate for a slight salinity decrease because of increased admixture of SSW during glacial stages. Dwyer et al. [38] postulated a similar Late Pliocene ice volume increase by 0.4‰. For comparison, the present ice volume on Greenland corresponds to an equivalent of 0.06‰ $\delta^{18}O$ equal to ~7 m sea level [41]. At DSDP Sites 609 and 610 the $\delta^{18}O$ increase from MIS G16–G10 matches the start of long-term IRD discharge in the northern North Atlantic, recording the general build-up of NHG, but precedes the final "climate crash" 2.74 Ma. Finally, at 2.82 Ma (immense IRD spike at MIS G10; Fig. 3a) the resulting sea level drop over glacial stages G16–G10 had progressed that far (Δ40–45 m) that it produced a positive feedback on the closure of the CAS which then were very shallow.

During the transient glacial stages of sea level lowstand the Panama Isthmus probably dried up completely, but was breached once again during interglacial stages. Indeed this conceptual model is strongly supported by the antiphasing of glacial-to-interglacial SST oscillations on both sides of the Panama Isthmus, an anomaly that first appeared at 2.82 Ma (coeval with the sudden great American faunal interchange [42]), reappeared after 2.65 Ma, and continued beyond 2.5 Ma [3, Tiedemann, pers. comm.].

At intermediate depth (1700 m), ODP 984 records the evolution of LSW, a component of Upper NADW. Here, glacial benthic $\delta^{18}O$ maxima jumped only once during MIS G8–G4, from 3.6‰ to 4.2‰ (Fig. 2b). This abrupt 0.6‰ increase matches a similar 0.5‰ shift at DSDP 609 at 3900 m depth, a shift that does not parallel a further DWT decrease (Fig. 3d and e) and thus documents a second major expansion of global ice volume by approximately 45 m sea level

Fig. 3. Paleoclimatic records for the Pliocene North Atlantic. (a) SSS anomaly (Caribbean– East Pacific) record of the final gradual closure of the CAS [3] and IRD record of NHG from ODP 907 (Iceland Plateau) [29] with new age model [30] based on tephra stratigraphy in number/g dry sediment. *Marks first synglacial closure of CAS. (b) Mg/Ca-SST from ODP 984 and DSDP 609. Red dots are data obtained from *G. bulloides*, orange dots are data obtained from *N. atlantica.* (c) Planktic $\delta^{18}O$ curves from ODP 984 and DSDP 609. Dark blue dots are data obtained from *G. bulloides*, light blue dots from *N. atlantica*. (d) Benthic $\delta^{18}O$ records from DSDP 610 [12] (*Cibicides spp*.) and DSDP 609 (*C. wuellerstorfi, C. pachyderma, U. peregrina, O. tener* adjusted to *U. peregrina*). Numbers 101, 103, G1, etc. are interglacial Marine Isotope Stages. DSDP 609 data from MIS G17 to M2 were kindly provided by R. Tiedemann, Kiel. (e) Mg/Ca-based DWT record from S. 609, averaged values (see Methods). (f) Number of benthic foraminifera *Cassidulina teretis*/10 g dry sediment, a species characteristic of low nutrient input and high seasonality [59]. (g) Benthic $\delta^{13}C$ records from ODP 984 (*C. wuellerstorfi* and *O. tener*), DSDP 610 [12] (*C. wuellerstorfi*), and from DSDP 609 (*C. wuellerstorfi* and *C. pachyderma*). Horizontal arrows mark Upper Pliocene water mass boundaries between SSW and LSW/LNADW [55]. Times of major change (2.95–2.82 Ma and 2.75–2.72 Ma) are highlighted. Labelled arrows outline major long-term trends (on top of glacial-to-interglacial variability).

equivalent, also recorded in the increase of IRD (Fig. 3a). In total, the sea level may have been lowered by 90 m with the onset of NHG. During MIS G6, the benthic $\delta^{18}O$ signal at ODP 984 may provide a striking new insight into the scenario of the great "climate crash". It appears to be linked to a major southward shift of the sites of NADW formation per analogy to that of the Last Glacial Maximum [43,44], that is from the Nordic Seas to the south of Iceland. Due to a lack of benthic foraminifers glacial MIS G16 to G10 are insufficiently recovered at ODP 984 to pick the first expansion of global ice volume between MIS G16 and G10.

3.2. Increase in poleward heat and salt transport in the North Atlantic

A long-term warming of the North Atlantic and accordingly, an increased poleward heat transport by the Gulf Stream–NAC system around 3 Ma along with the final closure of the CAS was first suggested by means of ostracodes and planktic foraminiferal assemblages from coastal deposits of the eastern U.S. and northern Iceland [45]. This conclusion was supported by various recent GCM models [46,47] which independently predict a SST rise of 2–3 °C for the northern North Atlantic.

With Mg/Ca-paleothermometry on the planktic foraminifera *G. bulloides* we now succeeded to generate two high-precision (±0.5–1.0 °C) SST records of the NAC system with 300–600 yrs resolution. Accordingly, early Late Pliocene SST varied at ODP 984 (IC) during summer from 6.7–14.0 °C and further southeast, at DSDP 609 (NAC) from 8.5–19.1 °C (Fig. 2b), with Mg/Ca ratios ranging from 0.9–2.1 and 1.2–3.7 mmol/mol. In general, interglacial temperatures then were 7–8 °C warmer than today [48]. Pliocene glacial SST were as mild as interglacial SSTs today, i.e. ~4 °C warmer than during the last glacial [49].

Most striking is the pronounced interglacial SST rise by 2–3 °C from MIS G15 to G11 (2.95–2.83 Ma). The final high SST level persisted over all subsequent interglacial stages until at least 2.5 Ma (ODP 984; not yet analyzed at DSDP 609). At DSDP 609 short lasting SST maxima similar to those at 2.85 Ma were also recorded earlier, at MIS KM1 and M1 (3.12 Ma and >3.26 Ma; Fig. 3b). The outlined great warming around 2.85 Ma was felt as far north as 80°N, as recorded by the warm-water dinoflagellate *Operculodinium centrocarpum* at ODP 911, northwest of Svålbard [50]. In the subartic North Pacific (ODP 882) a 1‰ decrease in planktic $\delta^{18}O$ suggests a similar 4 °C increase in SST from 2.85–2.77 Ma [31], prior to MIS G6, however, slightly subsequent to the great North Atlantic warming. The link to the North Atlantic is not yet understood.

Most likely, the great warming at 2.95–2.83 Ma and its precursors reflect an intensified poleward heat transport and meridional turnover of the ocean, events that went along with a significant increase in the discharge of IRD in the Greenland Sea (ODP 907) and a major cooling of deepwater during subsequent glacial stages. However, coeval interglacial planktic $\delta^{18}O$ values at ODP 984 and DSDP 609 (Fig. 3c) did not get depleted by 0.45–0.70‰ during this time, as was expected from the 2–3 °C warming. This absent ^{18}O depletion reflects a major increase in seawater $\delta^{18}O$, which in turn documents both a coeval amplification of the global $\delta^{18}O$ ice effect (0.2–0.4‰ ?) plus an increase in SSS by 0.2–0.4 psu, resulting from an enhanced salt transport in the Gulf Stream-NAC system. This trend was predicted by the modelers for the final closure of the CAS.

In addition, our new evidence for a 100-ky long coeval increase in SST and IRD (Fig. 3a and b) suggests that the interglacial (but not glacial) warming of the North Atlantic has much enlarged the supply of atmospheric moisture to high altitudes at northern high latitudes to initiate NHG. Indeed, high-latitudes vegetation patterns in Eurasia [51] reflect a distinct warming and moistening over this critical period. Accordingly, we follow the "snow gun hypothesis" [52] in assuming that this increase must have been large enough to overcome the opposed effect of the interglacial temperature rise that have enhanced ice melt, different from the reasoning of Berger and Wefer [53]. These processes occurred on top of a transient phase of increased Earth obliquity 3.0–2.3 Ma, which resulted in cooler summer climate.

However, the records of Atlantic THC do not reveal any particular (antecedent and/or coeval) events linked to the final "climate crash" of MIS G6, the second step of rapid climate deterioration. Since our records suffer from coring gaps and a lack of foraminifera tests in the pertinent glacial sections, we found no coeval, only a subsequent IRD rise and no increase

in SST, only an increase in benthic $\delta^{18}O$ that correspond to an additional ice volume equivalent of >45-m sea level drop. Possibly, this second step of climate deterioration was linked to thermohaline events in the northern North Pacific (*sensu* [31,54]), which recently were also explained by GCM modeling as effects of the final closure of the CAS [55].

Unfortunately, present GCM models appear unsatisfactory to predict precisely the conditions of the atmospheric water cycle, necessary to build-up continental ice sheets in the Late Pliocene. They either show a Greenland ice sheet already prior to the great North Atlantic warming [47] and/or do not succeed to generate the proper preconditioning of the climate system to build up a new ice sheet specific for the times approx. 2.92–2.83 Ma—independent of short-term differential amplitudes of orbital forcing [46].

3.3. Replacement of NADW during glacials by SSW

After 2.85 Ma DWT cooled from ~2 °C almost down to the freezing point (−1.8 °C) during glacial stages subsequent to MIS G12 at DSDP 609. This cooling either reflects an enhanced incursion of cold SSW and thus, a relative shoaling of NADW, or an increased contribution and/or cooling of northern high-latitude deepwater sources. Epibenthic $\delta^{13}C$ records, a proxy for deepwater ventilation at DSDP 609 and DSDP 610 (Fig. 3g) show a gradual $\delta^{13}C$ increase by 0.25–0.3‰ during interglacial stages G17 to G13, finally reaching 1.2–1.4‰. This high ventilation level forms a clear tracer of LNADW, whereas low $\delta^{13}C$ values of 0.3‰ and less, which are confined to short-lasting glacial stages (KM2, G22, and from G18 onwards) record short-term incursions of SSW originating from the Antarctic Circumpolar Current [56,57]. Moreover, the gradual increase in NADW ventilation from ~2.95 Ma to ~2.87 Ma reflects an enhanced meridional turnover rate during interglacial stages, which is in harmony with the prominent surface warming of the northeast Atlantic (Fig. 3b). Enhanced interglacial velocities of LNADW were also reported from various sites along the West Atlantic margin from 3.20–2.75 Ma [58]. Moreover, enhanced NADW formation led to improved carbonate preservation in the Nordic Seas during this time [59]. Subsequent to MIS G9, interglacial epibenthic $\delta^{13}C$ values at DSDP 610 again returned to the level prior to MIS G17, possibly reflecting a THC then slightly reduced.

Unfortunately, the highly fragmentary benthic $\delta^{13}C$ record of ODP 984 (1660 m) (not shown) does not reveal any significant trend in the variations of LSW which today and during the last glacial constitutes most of the Upper NADW. However, increased abundance of *C. teretis* subsequent to MIS G7 (Fig. 3f), may serve as robust tracer of LSW/Upper NADW during glacial and stadial conditions [60]. This trend may document a shift of deepwater convection cells from the Nordic Seas to the south of Iceland, as we already deduced from the benthic $\delta^{18}O$ record (Fig. 2b).

4. Conclusions

In summary, we find clear evidence based on IRD, SST, DWT, paleoproductivity, and deepwater ventilation records for an interglacial intensification of North Atlantic THC at 2.95–2.82 Ma (MIS G17–G11). This process has followed and probably accentuated the final closure of the CAS [3]. Moreover, it has promoted an increase in evaporation and poleward moisture transport from the North Atlantic as proposed by Haug and Tiedemann [2]. Beyond a short-term increase in Earth obliquity periods, increased moisture advection apparently has overcome the effects of interglacial warming and thus supported the fast build-up of continental ice sheets as documented by coeval IRD supply (Fig. 3a), as proposed by the "snow gun hypothesis" [52]. Finally, increased moisture advection to high latitudes has enhanced Siberian fluvial runoff and the formation of Arctic sea ice [9] and albedo, hence provided further support for the build-up of North Polar ice sheets. This conclusion neglects a potential global decrease in atmospheric pCO_2 as potential factor driving the onset of NHG [61] because Pliocene changes in pCO_2 actually observed are insignificant [62,63].

Subsequent to the major interglacial North Atlantic warming and first build-up of NHG 2.82 Ma (MIS G10), it took about 80,000 yrs (approximately two obliquity cycles) to arrive at the final "climate crash" during glacial MIS G6, when Quaternary-style [64] climate cycles were fully established,

sea level dropped further by 45 m, and floral and faunal provinces were rapidly reorganized on a global scale.

Acknowledgments

We gratefully acknowledge D. Pak and G. L. Paradis who helped with Mg/Ca analyses in Santa Barbara, moreover N. Gehre and K. Kißling in Kiel. H. Gebhardt contributed to our species taxonomy at DSDP 609. N. Andersen, H. Heckt and H.H. Cordt helped with stable-isotope analyses. We thank many Kiel students for tedious but careful sample preparation. The IODP Bremen and East Coast Repositories are acknowledged for sampling assistance. The DSDP 609 isotopic record in part was kindly provided by R. Tiedemann, Kiel. A. Schmittner helped commenting on an early manuscript version; G. Haug contributed a lot to the quality of this paper by his critical review; A. Holbourn improved on our English wording. This work was supported by the Deutsche Forschungsgemeinschaft (DFG) within the Kiel Research Unit "Ocean Gateways".

Data available on www.pangaea.de/PangaVista?query=@Ref26496.

References

[1] A.C. Ravelo, D.H. Andreasen, M. Lyle, A.O. Lyle, M.W. Wara, Regional climate shifts caused by gradual global cooling in the Pliocene epoch, Nature 429 (2004) 263–267.

[2] G.H. Haug, R. Tiedemann, Effect of the formation of the Isthmus of Panama on Atlantic Ocean thermohaline circulation, Nature 393 (1998) 673–676.

[3] J. Groeneveld, S. Steph, R. Tiedemann, D. Nürnberg, D. Garbe-Schönberg, G.H. Haug, The final closure of the Central American Seaway, Geology, in preparation.

[4] E. Maier-Reimer, U. Mikolajewicz, T. Crowley, Ocean general circulation model sensitivity experiment with an open Central American isthmus, Paleoceanography 5 (3) (1990) 349–366.

[5] S. Steph, Pliocene stratigraphy and the impact of Panama uplift on changes in Caribbean and tropical East Pacific upper ocean stratification (6–2.5 Ma). Thesis of Kiel University, 2005, 158 pp, 52 figs, 10 tables, 8 appendices.

[6] A.G. Coates, J.A. Obando, The geological evolution of the Central American Isthmus, in: J.B.C. Jackson, A.F. Budd, A.G. Coates (Eds.), Evolution and Environment in Tropical America, University of Chicago Press, Chicago, Illinois, 1996, pp. 21–56.

[7] G.H. Haug, R. Tiedemann, R. Zahn, A.C. Ravelo, Role of Panama Uplift on oceanic freshwater balance, Geology 29 (3) (2001) 207–210.

[8] L.D. Keigwin, Isotopic paleoceanography of the Caribbean and East Pacific: role of Panama Uplift in Late Neogene time, Science 217 (1982) 350–352.

[9] N.W. Driscoll, G.H. Haug, A short circuit in thermohaline circulation: a cause for Northern Hemisphere Glaciation? Science 282 (1998) 436–438.

[10] J.E.T. Channell, B. Lehman, Magnetic stratigraphy of North Atlantic sites 980–984, Proc. ODP, Sci. Res. 162 (1999) 113–130.

[11] W.E.N. Austin, J.R. Evans, Benthic foraminifera and sediment grain size variability at intermediate water depths in the Northeast Atlantic during the late Pliocene–early Pleistocene, Mar. Geol. 170 (2000) 423–441.

[12] H.F. Kleiven, E. Jansen, T. Fronval, T.M. Smith, Intensification of Northern Hemisphere glaciations in the circum Atlantic region (3.5–2.4 Ma) — ice-rafted detritus evidence, Paleogeogr. Paleoclimatol. Paleoecol. 184 (2002) 213–223.

[13] R. Tiedemann, M. Sarnthein, N.J. Shakleton, Astronomic timescale for the Pliocene Atlantic $\delta^{18}O$ and dust flux records of Ocean drilling Program site 659, Paleoceanography 9 (4) (1994) 619–638.

[14] J.-C. Duplessy, et al., ^{13}C record of benthic foraminifer in the last interglacial ocean: implications for the carbon cycle and the global deep water circulation, Quat. Res. 21 (1984) 225–243.

[15] M. Weinelt, G. Bartoli, H. Erlenkeuser, M. Sarnthein, Gateway-controlled decline of primary production in the northern North Atlantic at 2.74 Ma?, Mar. Micropaleontol. (submitted for publication).

[16] E. Jansen, U. Bleil, R. Henrich, L. Kringstad, B. Slettemark, Paleoenvironmental changes in the Norwegian Sea and the Northwest Atlantic during the last 2.8 m.y.: deep sea drilling project/ocean drilling program sites 610, 642, 643 and 644, Paleoceanography 3 (1988) 563–581.

[17] D.W. Graham, B.H. Corliss, M.L. Bender, L.D. Keigwin Jr., Carbon and oxygen isotopic disequilibria of recent deep-sea benthic foraminifera, Mar. Micropaleontol. 6 (1981) 483–497.

[18] P.A Martin, D.W. Lea, A simple evaluation of cleaning procedures on fossil benthic foraminiferal Mg/Ca, Geochem, Geosys. Geophys. 3 (2002) 8401.

[19] D. Garbe-Schönberg, J. Groeneveld, G. Bartoli, M. Sarnthein, C. Dullo. High-precision Mg/Ca and Sr/Ca ratios of biogenic carbonate and seawater by simultaneous ICP-OES, Geochem. Geosys. Geophys., in preparation.

[20] S. de Villiers, M. Greaves, H. Elderfield, An intensity ratio calibration method for the accurate determination of Mg/Ca and Sr/Ca of marine carbonates by ICP-AES, Geochem. Geosys. Geophys. 3 (2002).

[21] T.A. Mashiotta, D.W. Lea, H.J. Spero, Glacial-interglacial changes in Subantarctic sea surface temperature and $\delta^{18}O$-water using foraminiferal Mg, Earth Planet. Sci. Lett. 170 (1999) 417–432.

[22] M. Kucera, J.P. Kennett, Causes and consequences of a middle Pleistocene origin of the modern planktonic foraminifer *Neogloboquadrina pachyderma* sinistral, GSA Bull. 30 (6) (2002) 539–542.
[23] H. Elderfield, G. Ganssen, Past temperature and $\delta^{18}O$ of surface ocean waters inferred from Mg/Ca ratios, Nature 405 (2000) 442–445.
[24] P. Anand, H. Elderfield, M.H. Conte, Calibration of Mg/Ca thermometry in planktonic foraminifera from a sediment trap time series, Paleoceanography 18 (2) (2003) 1050.
[25] P.A. Martin, et al., Quaternary deep sea temperature histories derived from benthic foraminiferal Mg/Ca, Earth Planet. Sci. Lett. 198 (2002) 193–209.
[26] C.H. Lear, Y. Rosenthal, N. Slowey, Benthic foraminiferal Mg/Ca-paleothermometry: a revised core-top calibration, Geochim. Cosmochim. Acta 66 (19) (2002) 3375–3387.
[27] R.G.A. Fairbanks, 17,000-year glacio-eustatic sea level record: influence of glacial melting rates on the Younger Dryas event and deep-ocean circulation, Nature 342 (1989) 637–642.
[28] E. Jansen, J. Sjøhølm, Reconstruction of glaciation over the past 6 Myr from ice-borne deposits in the Norwegian Sea, Nature 349 (1991) 600–603.
[29] E. Jansen, T. Fronval, F. Ranck, J.E.T. Channell, Pliocene–Pleistocene ice rafting history and cyclicity in the Nordic Seas during the last 3.5 Myr, Paleoceanography 15 (2000) 709–721.
[30] C. Lacasse, P. van den Bogaard, Enhanced airborne dispersal of silicic tephras during the onset of Northern Hemisphere glaciations, from 6 to 0 Ma records of explosive volcanism and climate change in the subpolar North Atlantic, Geology 30 (7) (2002) 623–626.
[31] M.A. Maslin, G.H. Haug, M. Sarnthein, R. Tiedemann, The progressive intensification of northern hemisphere glaciation as seen from the North Pacific, Geol. Rundsch. 85 (1996) 452–465.
[32] R.C. Thunell, P. Belyea, Neogene planktonic foraminiferal biogeography of the Atlantic Ocean, Micropaleontology 28 (4) (1982) 381–398.
[33] T. Sato, S. Yuguchi, T. Takayama, K. Kameo, Drastic change in the geographical distribution of the cold-water nannofossil *Coccolithus pelagicus* (Wallich) Schiller at 2.74 Ma in the Late Pliocene, with special reference to glaciation in the Arctic Ocean, Mar. Micropaleontol. 52 (2004) 181–193.
[34] K. Kameo, T. Sato, Biogeography of Neogene calcareous nannofossils in the Caribbean and eastern equatorial Pacific-floral response to the emergence of the Isthmus of Panama, Mar. Micropaleontol. 39 (2000) 201–218.
[35] D. Schnitker, High resolution records of benthic foraminifera in the Late Neogene of the northeastern Atlantic, DSDP Init. Rept. 81 (1989) 611–622.
[36] C.H. Lear, H. Elderfield, P.A. Wilson, Cenozoic Deep-Sea temperatures and global ice volumes from Mg/Ca in benthic foraminiferal calcite, Science 287 (2000) 269–272.
[37] L.E. Lisiecki, M.E. Raymo, A Pliocene–Pleistocene stack of 57 globally distributed benthic $\delta^{18}O$ records, Paleoceanography 20 (2005) PA1003.
[38] G.S. Dwyer, et al., North Atlantic deepwater temperature change during the Late Pliocene and Late Quaternary climatic cycles, Science 270 (1995) 1347–1350.
[39] K. Billups, D.P. Schrag, Paleotemperatures and ice volume of the past 27 Myr revisited with paired Mg/Ca and $^{18}O/^{16}O$ measurements on benthic foraminifera, Paleoceanography 17 (2002) 1003–1014.
[40] C.H. Lear, Y. Rosenthal, J.D. Wright, The closing of a seaway: ocean water masses and global climate change, Earth Planet. Sci. Lett. 210 (2003) 425–436.
[41] J.M. Greogory, P. Huybrechts, S.C.B. Raper, Threatened loss of the Greenland ice-sheet, Nature 428 (2004) 616.
[42] S.D. Webb, The great American faunal interchange, in: A.G. Coates (Ed.), Central America: A Natural and Cultural History, Yale University Press, New Haven, 1997, pp. 97–122.
[43] J.-C. Duplessy, et al., Surface salinity reconstruction of the North Atlantic Ocean during the last glacial maximum, Oceanol. Acta 14 (4) (1991) 311–324.
[44] U. Pflaumann, et al., Glacial North Atlantic: sea-surface conditions reconstructed by GLAMAP 2000, Paleoceanography 18 (3) (2003) 1065.
[45] H.J. Dowsett, et al., Micropaleontological evidence for increased meridional heat transport in the North Atlantic Ocean during the Pliocene, Science 258 (1992) 1133–1135.
[46] A. Klocker, M. Prange, M. Schulz, Testing the influence of the Central American Seaway on orbitally forced northern hemisphere glaciation, Geophys. Res. Lett. 32 (2005) L03703.
[47] A. Schmittner, B. Schneider, Simulating the impact of the Panamanian seaway closure on ocean circulation, marine productivity and nutrient cycling, in preparation.
[48] S. Levitus, T. Boyer, World Ocean Atlas 1994, Temperatures. NOAA Atlas NESDIS4, 4, US. Department of Commerce, Washington, D. C., 1994.
[49] S. van Kreveld, et al., Potential links between surging ice sheets, circulation changes, and the Dansgaard–Oeschger cycles in the Irminger Sea, 60–18 kyr, Paleoceanography 15 (2000) 425–442.
[50] J. Knies, J. Matthiessen, C. Vogt, R. Stein, Evidence of "Mid-Pliocene (~3 Ma) global warmth" in the eastern Artic Ocean and implications for the Svålbard/Barents Sea ice sheet during the late Pliocene and early Pleistocene (~3–1.7 Ma), Boreas 31 (2002) 82–93.
[51] Baikal Drilling project BDP-96 (Leg II) Members, Continuous paleoclimate record recovered for last 5 million years, EOS 78 (51) (1997) 597–601.
[52] M.L. Prentice, R.K. Matthews, Tertiary Ice Sheet Dynamics: the snow gun hypothesis, J. Geophys. Res. 96 (1991) 6811–6827.
[53] W. Berger, G. Wefer, Expeditions into the Past: paleoceanographic studies in the South Atlantic, in: G. Wefer, W. Berger, G. Siedler, D. Webb (Eds.), The South Atlantic: Present and Past Circulation, Springer-Verlag, Berlin, 1996, pp. 363–410.
[54] G.H. Haug, et al., North Pacific seasonality and the glaciation of North America 2.7 million years ago, Nature 433 (2005) 821–825.

[55] T. Motoi, W.-L. Chan, S. Minobe, H. Sumata, North Pacific halocline and cold climate induced by Panamanian Gateway closure in a coupled ocean-atmosphere GCM, Geophys. Res. Lett. 32 (2005) L10618, doi:10.1029/2005GL022844.
[56] A.C. Ravelo, D.H. Andreasen, Enhanced circulation during a warm climate, Geophys. Res. Lett. 27 (7) (2000) 1001–1004.
[57] M. Sarnthein, et al., Changes in east Atlantic deepwater circulation over the last 30,000 years: eight time slice reconstructions, Paleoceanography 9 (2) (1994) 209–267.
[58] M. Gröger, R. Henrich, T. Bickert, Variability of silt grain size and planktic foraminiferal preservation in Plio/Pleistocene sediments from the western equatorial Altlantic and Caribbean, Mar. Geol. 201 (2003) 307–320.
[59] R. Henrich, K.-H. Baumann, R. Huber, H. Meggers, Carbonate preservation records of the past 3 Myr in the Norwegian–Greenland Sea and the northern North Atlantic: implications for the history of NADW production, Mar. Geol. 184 (2002) 17–39.
[60] A.E. Jennings, G. Helgadottir, Foraminiferal assemblages from the fjords and shelf of eastern Greenland, J. Foraminiferal Res. 24 (1994) 123–144.
[61] T.J. Crowley, Modeling pliocene warmth, Quat. Sci. Rev. 10 (1991) 275–282.
[62] M.E. Raymo, B. Grant, M. Horowitz, G.H. Rau, Mid-Pliocene warmth: stronger greenhouse and stronger conveyor, Mar. Micropaleontol. 27 (1996) 313–326.
[63] J. Zachos, M. Pagani, L. Sloan, E. Thomas, K. Billups, Trends, rhythms, and aberrations in global climate 65 Ma to present, Science 292 (2001) 686–693.
[64] B. Pillans, T. Naish, Defining the quaternary, Quat. Sci. Rev. 23 (2004) 2271–2282.